Principle of a submerged freeze gripper for micro-assembly.

Beatriz Lopez-Walle, Michaël Gauthier, Nicolas Chaillet

Principle of a submerged freeze gripper for micro-assembly

Beatriz López-Walle, Michaël Gauthier (corresponding author), *IEEE Member*, and Nicolas Chaillet, *IEEE Member*

***Abstract*—The development of reliable and repeatable strategies to manipulate and assemble micro-objects lies in the efficiency, reliability and precision of the handling processes. In this paper, we propose a thermal based microgripper working in an aqueous medium. Manipulating and assembling in liquid surroundings can indeed be more efficient than in dry conditions. A comparative analysis on the impact of dry and liquid media on surface forces, contact forces and hydrodynamic forces is shown. In addition, ice grippers represent flexible manipulation solutions. Nevertheless, when micromanipulation tasks are performed in air, capillary forces can drastically perturb the release. Our submerged freeze microgripper exploits the liquid surroundings to generate an ice droplet to catch micro-objects, and to avoid capillary forces during the release. The thermal principle, the first microgripper prototype, an ice generation simulation, and the first tests are presented. The main objective is to validate the manipulation principle. Further works will be focused on control and optimization of the ice generation and the miniaturization of the system.**

***Index Terms*—Ice gripper, Peltier effect, micromanipulator.**

I. Introduction

MANIPULATING objects whose typical size corresponds to the so-called microworld, i.e. typically between one micrometer and one millimeter, requires particularly efficient, reliable and precise handling processes. During the last years, numerous grip principles have been studied and developed to perform these main tasks: picking up, moving and releasing the manipulated micro-object. Most of them are able to pick and move objects with acceptable performance; in contrast, releasing them with good reliability and high accuracy still remains a critical problem [1].

The release phase is strongly affected by surface forces, especially for objects under 100 micrometers [2]–[4]. A comparative analyse detailed in [5] clearly shows that surface forces (van der Waals force, electrostatic force) and contact force (pull-off force) reduce significantly in liquid medium [6]–[8]; capillary forces are completely cancelled in submerged conditions; and hydrodynamic force increases in submerged environment. Then, these phenomena reduce drastically the adhesion and electrostatic perturbations in one hand; and the loss of micro-objects, because their maximal velocity is limited by the hydrodynamic force, in the other hand. Performing manipulation tasks in submerged conditions represents a very promising approach.

In this paper, we propose a micromanipulation principle adapted to the liquid medium. The objective of this paper is to validate this principle. The handling strategy is shown in Fig. 1. In the first step, the gripper approaches the object without touching it. In the second step, an ice droplet is generated adjacent to a small part of the object. The object can be then positioned. In the last step, the ice droplet thaws mixing with the aqueous medium and the object is released without any influence of capillary forces.

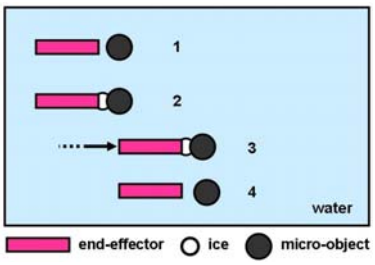

Fig. 1. Handling Strategy: (1) the micro-gripper approaches, (2) an ice droplet is generated and catches the object, (3) the object is manipulated, (4) the ice thaws and the object is liberated.

Ice grippers have been used for manipulating objects in air, as described in [9]–[12]. The dimensions of gripped objects are typically bigger than 200 μm and the main applications are optical, mechanical or electrical micro-components assembly [11]. Their thermal principle is based either on Joule-Thompson effect, or Peltier effect. Water must be provided by an external device because they work in air, and capillary forces appear during the release because water does not evaporate completely. Then they have to be combined with other release strategies to detach manipulated objects. In addition, they must work with particular environmental conditions like low temperature and low humidity [9], [13]. The miniaturization of these grippers is limited by the release difficulties.

Traditionally, standard gripping systems, like friction tweezers or vacuum grippers, are used for grasping micro-objects. Simple tweezers can be applied in many applica-

Authors are with AS2M/Institut FEMTO-ST, UMR CNRS 6174 - ENSMM - UFC, 24 rue Savary, 25000 Besançon, France - Tel: +33(0)381402810 Fax:+33(0)381402809 e-mail: michael.gauthier@femto-st.fr.

Submitted paper as Short Paper to IEEE Transactions on Robotics.

tions, but usually requires to design specific end-effectors for each type of micromanipulated objects. Nevertheless, the adhesion perturbations increase when part size diminishes and force control is required for fragile components. In addition, it is necessary to have at least two accessible surfaces to grasp parts [9], [13], [14]. Vacuum grippers have weak mechanical constraints. They need only one accessible surface but are limited to flat-side components or components with simple 3D shapes. Their cycle time is generally very short ($< 0.1\ s$) [9], [14]. Features of capillary grippers [15]–[17] are similar to cryogenic grippers, but their miniaturization is limited because of adhesion perturbations during the release phase.

The handling abilities of the cryogenic grippers are almost independent of the object shape. They provide high holding forces but local stresses can be also very high, damaging delicate micro-objects. It is recommended that the manipulated micro-component can with stand low temperatures and should not be liable to rust. Inserting it into the water container, recuperating it, and drying it will be analysed. In addition, the water temperature must be relatively close to the fusion temperature ($< 10\ ^oC$).

The submerged freeze gripper proposed in this paper, profits from the advantages of submerged manipulation particularly the cancellation of capillary force. Consequently, it can be extended to smaller objects below 100 μm in typical size.

This paper presents the submerged freeze gripper principle, and the technical and physical characteristics of the first prototype in section II. The dynamical modelling of the ice generation is described in section III. Then, the first experimentations are given in section IV.

II. The Submerged Freeze Gripper

We developed a first prototype of the submerged freeze gripper. Its principle is based on the Peltier effect, and its physical and technical characteristics are presented in this section.

A. Submerged Freeze Gripper Principle

The submerged freeze gripper utilizes the aqueous environment to create an ice droplet. The energy for freezing water is provided by two Peltier thermoelectric components.

A Peltier module is the association of bismuth-telluride p and n-doped semiconductors connected electrically in series and thermally in parallel. It provides a heat flux which is proportional to the electrical current applied to the module and the direction of the heat flow depends on the direction of the current. The difference of temperatures caused by the heat transfer imposes a cold face and a hot face. The hot face must be associated to a heat sink in order to dissipate the heat flux.

As illustrated in Fig. 2, the submerged freeze system consists of two Peltier module stages, and a forced convection system. The first stage contains a Peltier micromodule named MicroPelt (μP). The end-effector is directly attached to its cold side. By this way, the MicroPelt can cool it and consequently generates the ice droplet on its acting part. The freezing process increases the temperature of the MicroPelt's hot face. An important convection heat flow appears between the cold and the hot faces of the MicroPelt. This flow can warm up the system (liquid, gripper and Peltier micromodule). To actively decrease the temperature at the MicroPelt's heat sink, a second Peltier element is connected. We called it MiniPeltier (mP). The temperature of its hot face must be constant to optimize its performance: it is maintained at the ambient temperature by forced convection using a liquid cooling system. This last is not directly used to the MicroPelt's hot face because it is a bulky system. The MiniPeltier enables to design a compact submerged freeze gripper. The end-effector and the MicroPelt are completely submerged and electrically insulated. The MiniPeltier and the cooling liquid system stay in air to dissipate heat outside water.

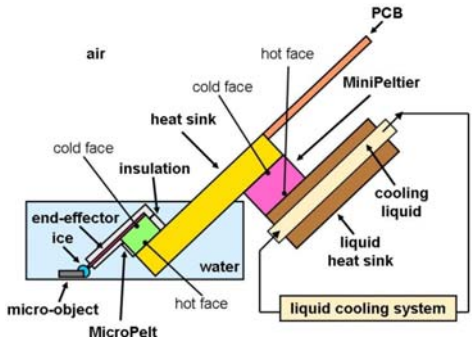

Fig. 2. Submerged Freeze System Principle.

B. Physical and Technical Characteristics

The first prototype of the submerged freeze gripper and the design of the end-effector is shown in Fig. 3.

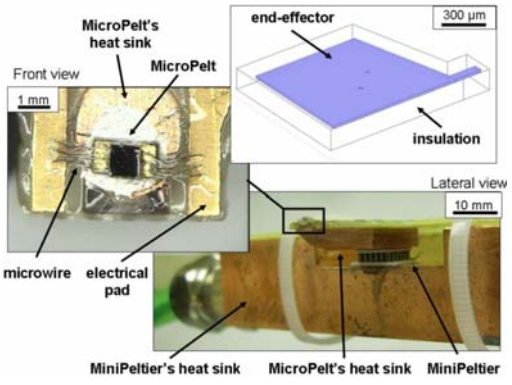

Fig. 3. Experimental freeze gripper and design of the end-effector.

The MicroPelt (Infineon Technologies AG) has as dimensions $720 \times 720 \times 428\ \mu m^3$. Its hot face is fastened to a copper heat sink with silver glue that provides excellent thermal conductivity. The MiniPeltier (Melcor FC0.6-18-05), whose dimensions are $6.2 \times 6.2 \times 2.4\ mm^3$, is fixed on its cold face to the MicroPelt's heat sink; and on its hot face to the copper liquid heat sink of the cooling liquid system. In both cases, we use liquid glue and thermal paste.

The liquid cooling system is a Thermaltake BigWater SE. Basically it consists of a container for 500 ml of cooling liquid, a 12 mm fan and a 12 V pump connected to the copper liquid heat sink. Its dimensions have not been yet optimized.

The 20 μm thick nickel end-effector is covered by a 20 μm thick SU-8 insulation layer. It has not been yet fabricated. A specific PCB has been fabricated to establish the electrical connections of both Peltier modules. Because of the very small dimensions of the MicroPelt, microwire-bonding technology is used for its connections.

III. Simulation of the Ice Generation

Dynamic simulations of the submerged freeze gripper allow examination of the ice droplet generation and shape in order to study and to validate the performance of the gripper.

As the Peltier elements are controlled by electrical currents, the ice droplet growth, named $Thick_{ice}$, depends thus on both MicroPelt's electrical current, $i_{\mu P}$, and MiniPeltier's electrical current, i_{mP}, as schematized in Fig. 4. The modelling of the 3D submerged freeze gripper has been performed using the finite element (FEM) software COMSOL Multiphysics 3.2. Fig. 5 shows this 3D FEM model. In one hand, passive elements (MicroPelt's heat sink, water, end-effector, and PCB support) have been directly modelled in the software. The following assumptions (based in experimental conditions) are made: (a) all the walls of the water container are thermally insulated; (b) heat convection occurs on the contact surface between water and air; (c) the liquid cooling system maintains the temperature of the MiniPeltier's hot face at air temperature, so the MiniPeltier's hot face temperature is assumed to be constant. On the other hand, active elements (i.e. Peltier modules) have been first mathematically modelled via the heat expressions at their cold and hot faces. Their dynamic behaviours can be neglected in comparison with the dynamic behaviours of the passive elements because of their small size. For this reason, only the Peltier modules' static behaviours were considered in the FEM model. Concerning the MiniPeltier, the temperature of the cold face is modelled directly by a function of its electric current, and the hot face temperature is considered constant at ambient temperature.

Considering one Peltier module, heat absorbed by the cold face Q_c and heat rejected by the hot face Q_h are related to Peltier coefficient α, electrical resistance R, thermal conductance k_P, electrical current supplied i, and

Fig. 4. Studied system for ice generation modelling.

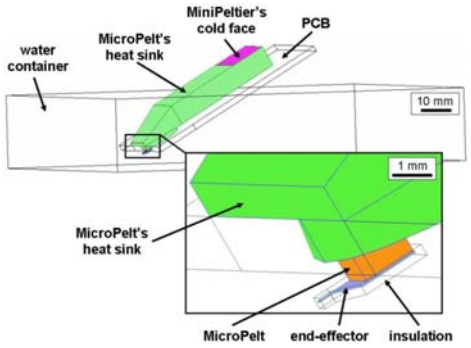

Fig. 5. 3D FEM model of the submerged freeze gripper.

temperature on cold and hot faces, T_c and T_h respectively. Their expressions can be written as:

$$Q_c = -\alpha T_c i + \frac{Ri^2}{2} + k_P(T_h - T_c) \quad (1)$$

$$Q_h = \alpha T_h i + \frac{Ri^2}{2} - k_P(T_h - T_c) \quad (2)$$

Table I gives the physical parameters for the MicroPelt and the MiniPeltier.

TABLE I
Physical Parameters for the Peltier Elements

Coefficient	**MicroPelt** (μP)	**MiniPeltier** (mP)
Peltier coefficient α (V/K)	$1.0 \cdot 10^{-3}$	$7.0 \cdot 10^{-3}$
Electrical resistance R (Ω)	0.2	1.158
Thermal conductance k_P (W/K)	0.0082	0.017

A. Electrical Currents of the Peltier Modules

The MicroPelt draws heat away to the end-effector in order to create the ice droplet. The temperature at the end-effector tip T_{ef} must be under 273 K. This temperature depends on the applied current $i_{\mu P}$. To ensure that the MicroPelt is able to induce the temperature $T_{ef} = 273\ K$, the temperature of its hot face must be slightly above 273 K. Because of the latter, the temperature of the MiniPeltier's cold side (T_{cmP}) will be maintained at 275 K. This temperature is sufficiently close to 273 K but it prevents the MicroPelt's heat sink from freezing.

To determine the range of $i_{\mu P}$ when the temperature on the end-effector tip, T_{ef}, is under 273 K, T_{cmP} is fixed at 275 K in the FEM modelling of the system, and we varied $i_{\mu P}$. Fig. 6 shows that T_{ef} is under 273 K when $i_{\mu P}$ is higher than 0.2 A. Further simulations demonstrate

that in case of setting $i_{\mu P}$ at 0.5 A, the cooling energy is sufficient to generate the ice droplet without losses through the end-effector insulation.

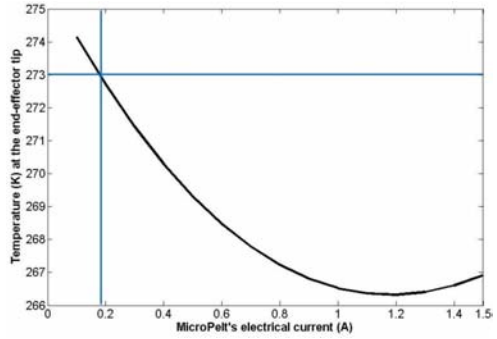

Fig. 6. Temperature at the active surface of the gripper as a function of MicroPelt's electrical current.

Knowing the MicroPelt's current, it is then possible to establish the value of the MiniPeltier's electrical current i_{mP} that ensures the temperature of its cold side T_{cmP} at 275 K as we referred above. In Fig. 7 we note that this temperature is reached around 0.9 A.

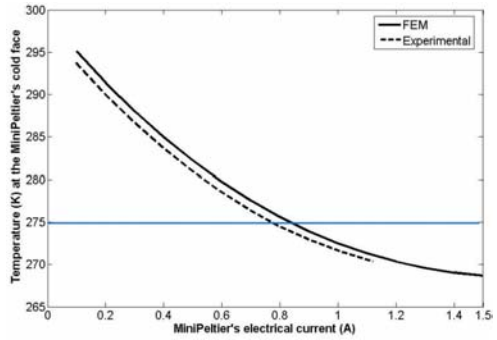

Fig. 7. Temperature at the MiniPeltier's cold face as a function of its electrical current.

The dynamic ice formation has been simulated on two surfaces: the MicroPelt's cold face and the end-effector's active surface. All of these simulations were performed as follows: (i) at first, i_{mP} is set at 0.9 A and i_{uP} at 0 A. A static simulation is done and the temperature T_{cmP} is thus establish at 275 K; (ii) a dynamic simulation let us observe the generation of the ice droplet as a function of time.

B. Forming the Ice Droplet on the MicroPelt's cold face

Without considering the end-effector, the ice droplet is generated on the cold face of the end-effector. We observed the ice generation at different times. The ice droplet is ellipsoidal in shape and its thickness depends on the cooling time. The longer the time, the bigger the ice droplet. The Fig. 8 represents the isotherms at 273 K at the 2D lateral section of the end-effector tip after 0.1 s, 1 s and 8 s. It indicates the boundary between the water surroundings and the ice droplet. As in the microworld surface effect becomes more prominent than volume effect, the energy required for the phase transformation (volume effect) can be neglected in comparison with the energy absorbed by the active surface of the end-effector. For example, the latent energy required to generate an ice volume after 5 seconds is 12 μW while the heat energy absorbed by the active surface of the end-effector is 265 μW. This last energy is most important than latent energy.

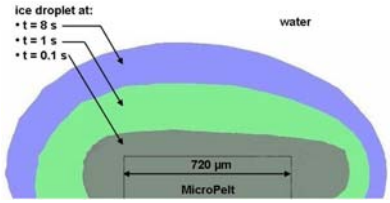

Fig. 8. 2D lateral view of the forming of the ice droplet at the MicroPelt's cold face.

Fig. 9 shows the ice thickness obtained by FEM simulations and measured experimentally as a function of time. We observe that the simulated ice droplet is generated faster than the experimental ice droplet until 1 second. Then, both results try to converge: at 3 seconds, measured thickness is 332 μm and simulated thickness is 556 μm and at 8 seconds, measured thickness is 507 μm and simulated thickness is 642 μm. The differences can be explained by the difficulty to identify the convection coefficient h between the MicroPelt's cold face and water. We assumed that this coefficient is constant: $h_{water} = 1500\ w/m^2K$.

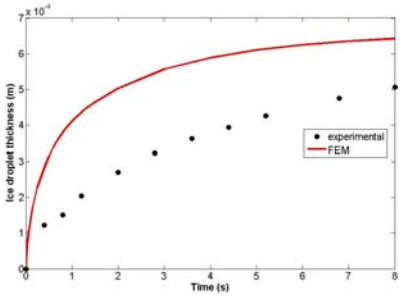

Fig. 9. Thickness of the ice droplet on the MicroPelt's cold face as a function of time.

C. Forming of the Ice Droplet on the End-effector's Active Surface

In order to reduce the size of ice droplet and consequently the time of the ice generation, we have simulated the dynamic ice generation on the end-effector's active surface. This observation was divided in three parts: first, without any manipulated object; second, picking up low thermal conductivity micro-objects; and third, picking up high thermal conductivity micro-objects.

Concerning the first case, Fig. 10 shows the isotherm at 273 K at the 2D lateral section of the end-effector tip after

0.1 s, 0.2 s and 0.5 s. This isotherm has not physical sense inside the SU-8 insulation layer and the end-effector.

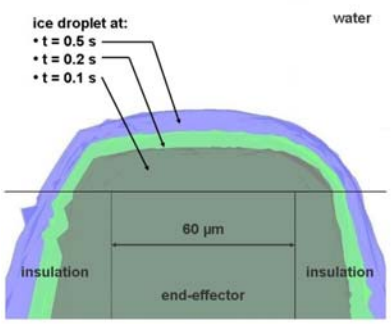

Fig. 10. 2D lateral view of the forming of the ice droplet on the end-effector's active surface.

D. Interaction with Low Thermal Conductivity Objects

Secondly, the performance of the submerged freeze gripper is studied simulating the grip phase of different low thermal conductivity micro-objects. In these cases the ice growth is not perturbed by the object. Fig. 11 illustrates the isotherm at 273 K at the 2D lateral section of the end-effector tip after cooling 0.1, 0.2 and 0.5 seconds. The object is a 70 μm diameter silica glass sphere, whose thermal conductivity coefficient is 1.38 W/mK. Based on this simulation, we conclude that the performance of the system is thus almost not perturbed by low thermal conductivity micro-objects.

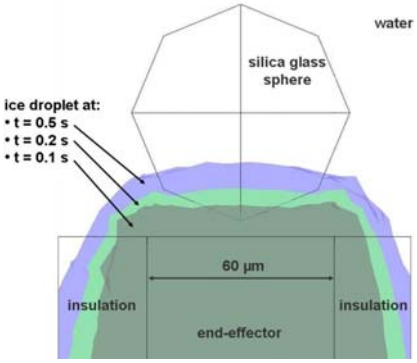

Fig. 11. 2D lateral view of the dynamic interaction between the ice droplet and a silica glass sphere.

E. Interaction with High Thermal Conductivity Objects

Finally, the pick up of different high thermal conductivity micro-objects with various shapes and materials has also been modelled. The ice generation is delayed compared to previous cases described above, as shown in Fig. 12. The object is a 70 μm diameter copper sphere. Its thermal conductivity coefficient is 400 W/mK.

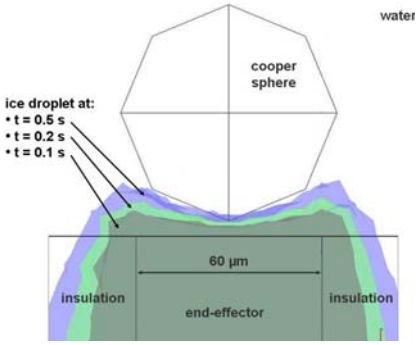

Fig. 12. 2D lateral view of the dynamic interaction between the ice droplet and a copper sphere.

F. Summary of the Ice Forming on the End-effector's Active Surface

3D FEM simulation was used to study and validate the submerged freeze gripper. Fig. 13 shows a complete water-ice-water cycle on the active surface of the end-effector with and without micro-objects. From 0 to 0.5 s, electrical currents are set as $i_{mP} = 0.9\ A$ and $i_{\mu P} = 0.5\ A$; otherwise i_{mP} stays constant at 0.9 A and $i_{\mu P} = -0.5\ A$.

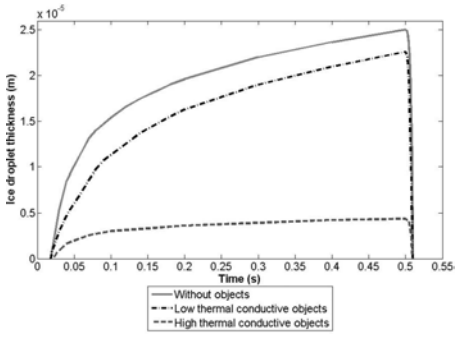

Fig. 13. Ice droplet formation and thawing in function of time.

Modelling the interactivity between the end-effector and different material objects confirms that manipulation is better for objects with a low thermal conductivity. In addition, reducing the active surface, the ice generation time, 0.1 s, is very short and can be compared with the reaction time of mechanical tweezers and vacuum grippers [18].

The Peltier elements' electrical currents obtained in this section have been used for experimental micromanipulations described in the following section.

IV. Experimentations

First experimentations using the prototype described in section II were performed. The objectives were to validate the performance of this new system and its reliability. For these first tests, the end-effector was not included. The active part is then the MicroPelt's cold face. These tests were realized in three steps: in the first one, the performance of the liquid cooling system and

the MiniPeltier has been verified; in the second one, the performance of the ice generation has been observed; in the third one, various micromanipulations have been completed.

A. The Liquid Cooling System

As previously explained, the liquid cooling system must maintain MiniPeltier's hot face temperature (T_{hmP}) at the ambient temperature (T_a). Experimentations verify that T_{hmP} remains almost constant when its electrical current (i_{mP}) ranges from 0 A to its maximal experimental value 1.1 A. The difference between T_a, i.e. 21.3 ^oC, and T_{hmP} is lower than 1.5 ^oC, as given in Table II. In this test, the MicroPelt has not been activated and the whole system stayed in air.

In addition, the temperature at the MiniPeltier's cold face (T_{cmP}) has been measured and is recorded on Fig. 7, in order to verify the FEM simulation. Both results, experimental and FEM, are very close.

TABLE II
STEADY STATE TEMPERATURE AT THE HOT FACE OF THE MINIPELTIER

Current i_{mP} (A)	0	0.39	0.79	1.10
Temperature T_{hmP} (^oC)	21.3	21.5	22.0	22.4

B. Ice Formation

To validate the performance of the ice formation, we realize some freezing-thawing cycles without any manipulated object. Fig. 14 shows measures obtained during this test. The temperatures are measured using microthermocouples and liquid is distilled water.

Before beginning this test, a pre-cooling phase is necessary to decrease the temperature of the MicroPelt's heat sink. During this phase, only the current in the MiniPeltier (i_{mP}) is applied and set constant at 0.9 A. When the temperature of the MicroPelt's hot face ($T_{h\mu P}$) is about 0,5 ^oC, the MicroPelt ($i_{\mu P}$) is activated setting its electrical current at 0.5 A. The temperature at the MicroPelt's cold face ($T_{c\mu P}$) locally diminishes until freezing point. At this point, $T_{c\mu P}$ increases because of the latent energy absorbed by the crystallization of water. As both electrical currents have no changes ($i_{mP} = 0.9$ A and $i_{\mu P} = 0.5$ A), ice droplet continues to grow and $T_{c\mu P}$ diminishes again. When $i_{\mu P}$ is inverted at -0.5 A, $T_{c\mu P}$ increases and ice thaws. This sequence has been repeated several times to validate the formation of the ice droplet.

C. Micromanipulations

Concerning the micromanipulations, Fig. 15 shows a frontal view of the tele-manipulation of a parallelepipedal silicon object whose dimensions are: $600 \times 600 \times 100$ μm^3. The micromanipulation is performed in distilled water. Temperatures are measured using microthermocouples.

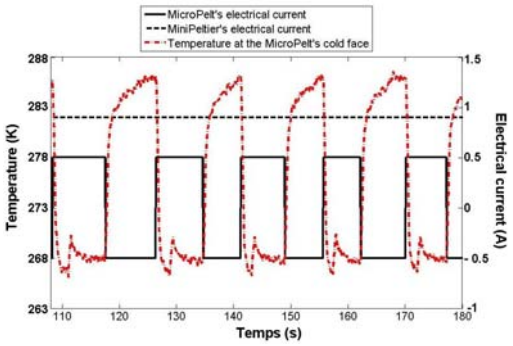

Fig. 14. Electrical current at the MicroPelt's cold face and electrical currents of the MicroPelt and the MiniPeltier as a function of time.

As in the test described above, a pre-cooling phase is also necessary (120 s) to decrease the temperature of the MicroPelt's hot face, T_{hmP}, until 0.5 ^oC. At this moment, the MicroPelt is positioned near the micro-object and its current ($i_{\mu P}$) is turned on at 0.5 A. The ice droplet is generated, around 4 μl in 3 s, which catches part of the object (Fig. 15b). The freeze gripper can thus displace it towards a new position (Fig. 15c). To release it, the MicroPelt's current is inverted at -0.5 A. The ice droplet starts to thaw on the end-effector's surface. The time necessary to thaw the ice on the end-effector surface is less than the sample time of the camera and cannot be measured. The object is released but a piece of ice stays around it. The ice droplet completely thaw in 7 s and melts with the medium, releasing the micro-object without adhesion perturbations (Fig. 15d). In this first test, we are waiting for the complete melting before moving the gripper.. The micromanipulation has been performed in 30 s. As previously mentioned, the cycle time for pick and release, obtained for optimal working conditions of the Peltier modules, is $3 + 7 = 10$ s. The rest of the time, i.e. 20 s of transportation time in this case, depends principally on operator's ability, or microgripper speed in case of full automation. Contrary to the cryogenics gripper in air, capillary forces do not perturb the release because the object and the MicroPelt are submerged.

The release of the micro-object is done either reversing the electrical current of the Peltier module or simply cancelling it. Reversing the direction is faster than cancelling electrical current, so we use this option.

The same experiment was successfully repeated several times. Consequently, the submerged freeze principle seems a promising approach to manipulate micro-objects.

Further works will be focused on the analyse of the heat exchanges between the end-effector and its surroundings, its design and its fabrication in order to manipulate objects sized under 100 μm.

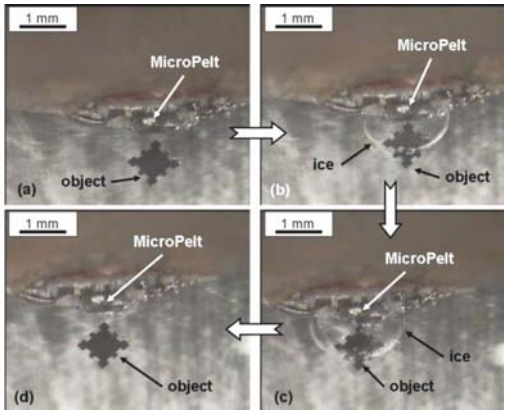

Fig. 15. Micromanipulation of a $600 \times 600 \times 100\ \mu m^3$ silicon object with the submerged freeze gripper.

V. Conclusion and future works

One of the principal challenges to execute efficient micromanipulations stays in performing handling strategies. These ones are permanently influenced by surfaces forces during the release phase. A comparative study of the dealings of dry and liquid media on surface forces, contact forces, and hydrodynamic forces show the advantages of the submerged micromanipulation. This new approach fosters us to develop an innovative micromanipulation strategy adapted to the aquatic medium. The submerged freeze gripper presented in this paper exploits the liquid medium to generate an ice droplet at the active part of the end-effector to pick up the micro-object. To release it, the ice is thawed without having any influence of the capillary force. A dynamical study by FEM simulations of the interaction between the gripper and objects with different thermal conductivities suggest that low thermal conductivity objects are recommended. The first experimentation shows the advantages of the liquid medium: pick and place tasks do not suffer adhesion perturbations. The submerged freeze gripper allows to execute reliable and flexible micromanipulation and micro-assembly tasks. Placement accuracy tests will be realized in further works.

To optimize the heat transfers involved in the handling process, maximizing the cooling energy to the end-effector, it should be necessary on one hand to improve the design of the submerged freeze gripper, and on the other hand to control the cold temperature of both Peltier elements via their electrical currents. The FEM modelling is not well-adapted to this last operation. So, we developed an equivalent model using electrical analogy. Further works will focus on verifying this model and miniaturizing the submerged freeze gripper to manipulate micro-objects sized under the 100 μm.

Acknowledgment

The authors would like to thank Micropelt GmbH for providing the MicroPelt Peltier coolers. This work is supported by the CONACYT Mexican National Council for Science and Technology, and the PRONOMIA 05-BLAN-0325-01 project granted by the ANR French National Research Agency.

References

[1] D. S. Haliyo and S. Régnier, "Advanced applications using micromad, the adhesion based dynamic micro-manipulator," in *Proc. of AIM*, Port Island, Japan, July 2003, pp. 880–885.

[2] M. Savia, Q. Zhou, and H. N. Koivo, "Simulating adhesion forces between arbitrarily shaped objects in micro/nano-handling operations," in *Proc. of IEEE/RSJ IROS*, Japan, 2004, pp. 1772–1727.

[3] Q. Zhou, B. Chang, and H. N. Koivo, "Ambient environment effects in micro/nano handling," in *Proc. of IWMF*, Shangai, China, October 2004, pp. 146–151.

[4] M. Gauthier, B. López-Walle, and C. Clévy, "Comparison between micro-objects manipulations in dry and liquid mediums," in *Proc. of CIRA*, Espoo, Finland, June 2005.

[5] M. Gauthier et al., "Analysis of forces for micromanipulations in dry and liquid media," *Journal of Micromechatronics*, vol. 3, no. 3-4, pp. 389–413, 2006.

[6] Z. Xu and R. H. Yoon, "The role of hydrophobic interactions in coagulation," *Journal of Colloid Interface Science*, vol. 44, no. 132, pp. 532–541, 1989.

[7] Z. Xu and R. H. Yoon, "A study of hydrophobic coagulation," *Journal of Colloid Interface Science*, vol. 45, no. 134, pp. 427–434, 1990.

[8] J. Israelachvili, *Intermolecular and surfaces forces*. Academic Press, 1991.

[9] A. Kochan, "European project develops "ice" gripper for micro-sized components," *Assembly Automation*, vol. 17, no. 2, pp. 114–115, 1997.

[10] J. Stephan and G. Seliger, "Handling with ice - the cryo-gripper, a new approach," *Assembly Automation*, vol. 19, no. 4, pp. 332–337, 1999.

[11] J. Liu, Y.-X. Zhou, and T.-H. Yu, "Freeze tweezer to manipulate mini/micro objects," *JMM*, vol. 14, no. 2, pp. 269–276, February 2004.

[12] D. Lang, M. Tichem, and S. Blom, "The investigation of intermediates for phase changing micro-gripping," in *Proc. of IWMF*, Besancon, France, October 2006.

[13] M. Tichem, D. Lang, and B. Karpuschewski, "A classification scheme for quantitative analysis of micro-grip principles," *Assembly Automation*, vol. 24, no. 1, pp. 88–93, 2004.

[14] S. C. Bou, A. Almansa, N. Balabanava, and Z. Rymuza, "Handling processes in microsystems technology," in *Proceedings of AIM*, Monterey, USA, July 2005.

[15] F. Biganzoli, I. Fassi, and C. Pagano, "Development of a gripping system based on a capillary force," in *Proc. of ISATP*, Canada, 2005, pp. 36–40.

[16] P. Lambert and A. Delchambre, "A study of capillary forces as a gripping principle," *Assembly automation*, vol. 25, no. 4, pp. 275–283, 2005.

[17] D. Schmid, S. Koelemeijer, J. Jacot, and P. Lambert, "Microchip assembly with capillary gripper," in *Proc. of IWMF*, France, 2006.

[18] S. Droz et al., "New generation of grippers for the manipulation of miniaturized components," in *Proc. of Mechatronics*, Besançon, France, October 2001, pp. 572–575.